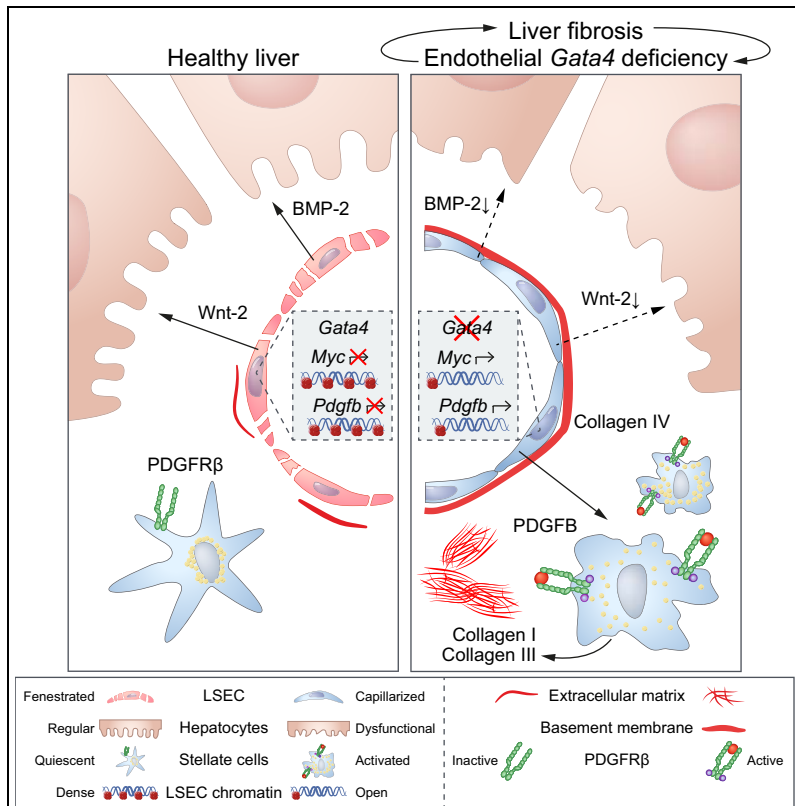


Endothelial GATA4 controls liver fibrosis and regeneration by preventing a pathogenic switch in angiocrine signaling

Graphical abstract



Authors

Manuel Winkler, Theresa Staniczek, Sina Wietje Kürschner, ..., Cyrill Géraud, Philipp-Sebastian Koch, Sergij Goerdt

Correspondence

manuel.winkler@medma.uni-heidelberg.de (M. Winkler), philipp.koch@umm.de (P.-S. Koch).

Lay summary

The liver vasculature is supposed to play a major role in the development of liver fibrosis and cirrhosis, which can lead to liver failure and liver cancer. Herein, we discovered that structural and transcriptional changes induced by genetic deletion of the transcription factor GATA4 in the hepatic endothelium were sufficient to cause liver fibrosis. Activation of the transcription factor MYC and *de novo* expression of the “angiocrine” growth factor PDGFB were identified as downstream drivers of fibrosis and as potential therapeutic targets for this potentially fatal disease.

Highlights

- Genetic endothelial *Gata4* deletion leads to liver fibrosis and hepatopathy.
- *Gata4* deficiency causes profibrotic angiocrine signaling via endothelial PDGFB.
- Increased chromatin accessibility and activated MYC mediate *Pdgfb* expression in LSECs.
- Dietary liver fibrosis causes dysregulation of the endothelial GATA4/MYC/PDGFB axis.
- In human cirrhosis, single-cell data implicate the GATA4/PDGFB axis.



Endothelial GATA4 controls liver fibrosis and regeneration by preventing a pathogenic switch in angiocrine signaling

Manuel Winkler^{1,*†}, Theresa Staniczek^{1,†}, Sina Wietje Kürschner^{1,†}, Christian David Schmid^{1,†},
Hiltrud Schönhaber¹, Julio Cordero², Linda Kessler², Arthur Mathes², Carsten Sticht³,
Michelle Neßling⁴, Alexey Uvarovskii⁵, Simon Anders⁵, Xue-jun Zhang^{6,7}, Guido von Figura⁸,
Daniel Hartmann⁶, Carolin Mogler⁹, Gergana Dobreva², Kai Schledzewski¹, Cyril Géraud^{1,10,11,‡},
Philipp-Sebastian Koch^{1,11,*‡}, Sergij Goerdt^{1,11,‡}

¹Department of Dermatology, Venereology and Allergology, University Medical Center and Medical Faculty Mannheim, Heidelberg University, and Center of Excellence in Dermatology, Mannheim, Germany; ²Department of Anatomy and Developmental Biology, European Center for Angioscience, Medical Faculty Mannheim, Heidelberg University, Mannheim, Germany; ³Core Facility Next Generation Sequencing, Medical Faculty Mannheim, Heidelberg University, Mannheim, Germany; ⁴Central Unit Electron Microscopy, German Cancer Research Center (DKFZ), Heidelberg, Germany; ⁵Center for Molecular Biology (ZMBH), Heidelberg University, Heidelberg, Germany; ⁶Department of Surgery, School of Medicine, Klinikum rechts der Isar, Technical University of Munich, Munich, Germany; ⁷Department of Orthopedic Surgery, Zhongda Hospital, School of Medicine, Southeast University, Nanjing, China; ⁸II. Medical Clinic and Polyclinic, School of Medicine, Klinikum rechts der Isar, Technical University of Munich, Munich, Germany; ⁹Institute of Pathology, School of Medicine, Technical University of Munich, Munich, Germany; ¹⁰Section of Clinical and Molecular Dermatology, Department of Dermatology, Venereology and Allergology, University Medical Center and Medical Faculty Mannheim, Heidelberg University, Mannheim, Germany; ¹¹European Center for Angioscience, Medical Faculty Mannheim, Heidelberg University, Mannheim, Germany

Background & Aims: Angiocrine signaling by liver sinusoidal endothelial cells (LSECs) regulates hepatic functions such as growth, metabolic maturation, and regeneration. Recently, we identified GATA4 as the master regulator of LSEC specification during development. Herein, we studied the role of endothelial GATA4 in the adult liver and in hepatic pathogenesis.

Methods: We generated adult *Clec4g-icre^{tg/0} × Gata4^{fl/fl}* (*Gata4^{L-SEC-KO}*) mice with LSEC-specific depletion of *Gata4*. Livers were analyzed by histology, electron microscopy, immunohistochemistry/immunofluorescence, *in situ* hybridization, and LSECs were isolated for gene expression profiling, ChIP- and ATAC-sequencing. Partial hepatectomy was performed to assess regeneration. We used choline-deficient, l-amino acid-defined (CDAA) diet and chronic carbon tetrachloride exposure to model liver fibrosis. Human single cell RNA-seq data sets were analyzed for endothelial alterations in healthy and cirrhotic livers.

Results: Genetic *Gata4* deficiency in LSECs of adult mice caused perisinusoidal liver fibrosis, hepatopathy and impaired liver regeneration. Sinusoidal capillarization and LSEC-to-continuous endothelial transdifferentiation were accompanied by a

profibrotic angiocrine switch involving *de novo* endothelial expression of hepatic stellate cell-activating cytokine PDGFB. Increased chromatin accessibility and amplification by activated MYC mediated angiocrine *Pdgfb* expression. As observed in *Gata4^{LSEC-KO}* livers, CDAA diet-induced perisinusoidal liver fibrosis was associated with GATA4 repression, MYC activation and a profibrotic angiocrine switch in LSECs. Comparison of CDAA-fed *Gata4^{LSEC-KO}* and control mice demonstrated that endothelial GATA4 indeed protects against dietary-induced perisinusoidal liver fibrosis. In human cirrhotic livers, GATA4-positive LSECs and endothelial GATA4 target genes were reduced, while non-LSEC endothelial cells and MYC target genes including *PDGFB* were enriched.

Conclusions: Endothelial GATA4 protects against perisinusoidal liver fibrosis by repressing MYC activation and profibrotic angiocrine signaling at the chromatin level. Therapies targeting the GATA4/MYC/PDGFB/PDGFRβ axis offer a promising strategy for prevention and treatment of liver fibrosis.

Lay summary: The liver vasculature is supposed to play a major role in the development of liver fibrosis and cirrhosis, which can lead to liver failure and liver cancer. Herein, we discovered that structural and transcriptional changes induced by genetic deletion of the transcription factor GATA4 in the hepatic endothelium were sufficient to cause liver fibrosis. Activation of the transcription factor MYC and *de novo* expression of the “angiocrine” growth factor PDGFB were identified as downstream drivers of fibrosis and as potential therapeutic targets for this potentially fatal disease.

© 2020 European Association for the Study of the Liver. Published by Elsevier B.V. This is an open access article under the CC BY-NC-ND license (<http://creativecommons.org/licenses/by-nc-nd/4.0/>).

Keywords: Mice; Humans; Liver fibrosis; Liver sinusoidal endothelial cells; Endothelial cells; Liver regeneration; Chromatin; ATAC-Seq; CDAA; Hepatic stellate cells; Angiocrine signaling; Cytokines.

Received 7 April 2020; received in revised form 12 August 2020; accepted 25 August 2020; available online 9 September 2020

* Corresponding authors. Address: Department of Dermatology, Venereology and Allergology, University Medical Center and Medical Faculty Mannheim, Heidelberg University, Theodor-Kutzer-Ufer 1-3, 68167 Mannheim, Germany. Tel.: +49 621 383 2280. (M. Winkler) (P.-S. Koch).

E-mail addresses: manuel.winkler@medma.uni-heidelberg.de (M. Winkler), philipp.koch@umm.de (P.-S. Koch).

† These first authors contributed equally to the work: Manuel Winkler, Theresa Staniczek, Sina Wietje Kürschner, Christian David Schmid.

‡ These senior authors contributed equally to the work: Cyril Géraud, Philipp-Sebastian Koch, Sergij Goerdt.

<https://doi.org/10.1016/j.jhep.2020.08.033>

Introduction

Among the microvascular beds of different organs, the hepatic sinusoids are a prime model of structural and functional



ELSEVIER

angiodiversity.¹ Liver sinusoidal endothelial cells (LSECs) are discontinuous and exert specialized functions in regulating liver immunity² and inflammation, and by clearing a variety of blood factors from the circulation via endocytic receptors such as the mannose receptor, CD32b, LYVE-1, Stabilin-1 and Stabilin-2.³ In addition, LSECs are sub-specialized and seem to be co-zonated with hepatocytes allowing a spatially defined paracrine cross-talk between the cells in the hepatic vascular niche.⁴

LSEC-derived organ-specific cytokines, so called “angiocrine factors”, are involved in liver development, homeostasis and disease pathogenesis.⁵ Angiocrine BMP-2 and BMP-6 signaling regulates iron metabolism by controlling secretion of hepcidin from hepatocytes.⁶ Angiocrine Wnt-2, Wnt-9b and R-spondin-3 signaling towards pericentral hepatocytes is indispensable for liver growth and maturation as well as metabolic liver zonation and liver regeneration.^{7,8} Regarding angiocrine control of liver fibrosis, important endothelial signaling systems in toxic liver fibrosis and/or bile duct ligation are the VEGF/SDF-1/CXCR-4/CXCR-7/FGFR-1 pathway,⁹ the eNOS/sGC axis¹⁰ and S1P1 signaling. Notably, HB-EGF has recently been identified as an angiocrine factor that maintains hepatic stellate cell (HSC) quiescence and whose secretion in liver fibrosis is impaired due to a lack of proteolytic processing.¹¹ Conversely, HSC-derived signaling towards LSECs is also involved in regulating liver fibrosis.¹² Therefore, it seems important to further scrutinize LSEC-HSC crosstalk in the hepatic vascular niche to decipher the pathogenesis of liver fibrosis and to identify novel therapeutic targets.

In contrast, the molecular regulators driving organ-specific differentiation of LSECs have not yet been comprehensively elucidated. While ID-1, LXR- α , endothelial Notch signaling,¹³ KLF-2, and ERG¹⁴ contribute to the molecular differentiation program of LSECs, we have recently identified the transcription factor GATA4 as the molecular master regulator of LSEC specification during early liver development, wherein it controls embryonic stem cell migration and fetal hematopoiesis.¹⁵ Herein, we sought to analyze the role of endothelial GATA4 in the adult liver and in hepatic disease pathogenesis.

Materials and methods

Ethical compliance

The experimental protocols used in this study complied with national and international ethical guidelines and, in case of animal models, were approved by the animal welfare commission of the Regierungspräsidium Karlsruhe (Karlsruhe, Germany).

Animal models

Female and male mice aged 1 day to 12 months were used in this study. Mice were hosted under specific-pathogen-free conditions in single ventilated cages in a 12 h/12 h day/night cycle and fed *ad libitum* with a standard rodent diet (V1534-000, Ssniff, Soest, Germany) with free access to water. For the generation of LSEC-specific conditional knockout mice *Clec4g-cre* driver mice¹³ (C57BL/6N-Tg(*Clec4g-cre*)1.1Sgoe, MGI:6280453) were crossed to *Gata4* floxed mice (STOCK *Gata4*^{tm1.1Sad}/J, JAX:008194), bearing a loxP site downstream of exon 3 and a loxP site upstream of exon 5. Mice bearing the genotype *Clec4g-cre*^{tg/0} x *Gata4*^{f/f} indicating homozygous recombination were denoted as *Gata4*^{LSEC-KO}. Littermates bearing the genotypes *Clec4g-cre*^{0/0} x *Gata4*^{f/f} or *Clec4g-cre*^{0/0} x *Gata4*^{w/w} were used as controls. Genetic background analysis of crossed mice used in this study is

provided in Table S1. Wild-type C57BL/6N mice were purchased from Janvier Labs (Le Genest-Saint-Isle, France) and were habituated for at least 1 week in the local animal facility before the start of experiments.

Statistical analysis

Statistical analyses were performed using R 3.6.1¹⁶ and Prism 8 (GraphPad Software, La Jolla, CA, USA). Sample size determination was performed separately for each experiment according to experience from previous experiments using an α -level of 0.05 and a β -level of 0.2. For statistical testing Welch's *t* test, paired *t* test, one- or two-way ANOVA, Fisher's exact test, and Mann-Whitney *U* test were used. A *p* value of <0.05 was considered statistically significant. The appropriate statistical test was chosen according to the requirements of each test (e.g. normal distribution or equal variance). Normal distribution was assessed using the Shapiro-Wilk test, equal variance using the *F*-test of equality of variances.

Additional methodological details

For further information on animal models, LSEC isolation, microarray and ATAC-seq analysis, and other materials and methods, please refer to the CTAT table and supplementary information.

Results

Endothelial *Gata4* deficiency causes perisinusoidal liver fibrosis and hepatopathy

To investigate the role of endothelial GATA4 in the adult liver, we established a novel genetic model of *Gata4* deficiency in adult hepatic endothelium. As *Stab2*-cre-driven liver endothelial-selective *Gata4* deficiency leads to embryonic lethality in mice between E14.5 and E17.5,¹⁵ we used *Clec4g-cre* driver mice in which Cre is not fully active in liver endothelial cells until E17.5.¹³ *Clec4g-cre*^{tg/0} x *Gata4*^{f/f} (*Gata4*^{LSEC-KO}) mice were born at a normal Mendelian ratio and their life expectancy was not reduced (Fig. S1A and B). PCR analysis confirmed recombination of *Gata4* in the genome and on the mRNA level in *Gata4*^{LSEC-KO} mice (Fig. S1C and D).

Macroscopically, the livers of 3-month-old *Gata4*^{LSEC-KO} mice revealed signs of liver fibrosis (Fig. 1A). Liver weight and liver-to-body weight ratio were significantly reduced in *Gata4*^{LSEC-KO} mice (Fig. 1B, Fig. S1E). Upon histology and picrosirius red staining (PSR), *Gata4*^{LSEC-KO} mice showed marked perisinusoidal liver fibrosis without any signs of bridging fibrosis (Fig. 1C and D). Deposition of collagens type I, III and IV was demonstrated by immunohistochemical staining confirming increased extracellular matrix protein synthesis (Fig. 1C, Fig. S1F). Accordingly, procollagen III N-terminal propeptide (PIINP) levels were increased in the peripheral blood of *Gata4*-deficient mice (Fig. 1E). In liver fibrosis, HSCs are the main source of collagens. In *Gata4*^{LSEC-KO} mice, HSC activity was found to be increased as measured by a reverse transcription quantitative PCR (RT-qPCR) panel including *Acta2*, *Col1a1*, *Col3a1*, *Des* and *Pdgfb* (Fig. 1F). Moreover, the number of HSCs was increased as analyzed by *in situ* hybridization (ISH) of *Pdgfb* (Fig. 1G, H).

Basic liver function tests showed significant elevations of aspartate aminotransferase, alanine aminotransferase and glutamate dehydrogenase as well as reduction of whole serum protein in *Gata4*^{LSEC-KO} mice, indicating impaired hepatocyte integrity and function (Fig. 1J-L, Fig. S1G). Moreover, a

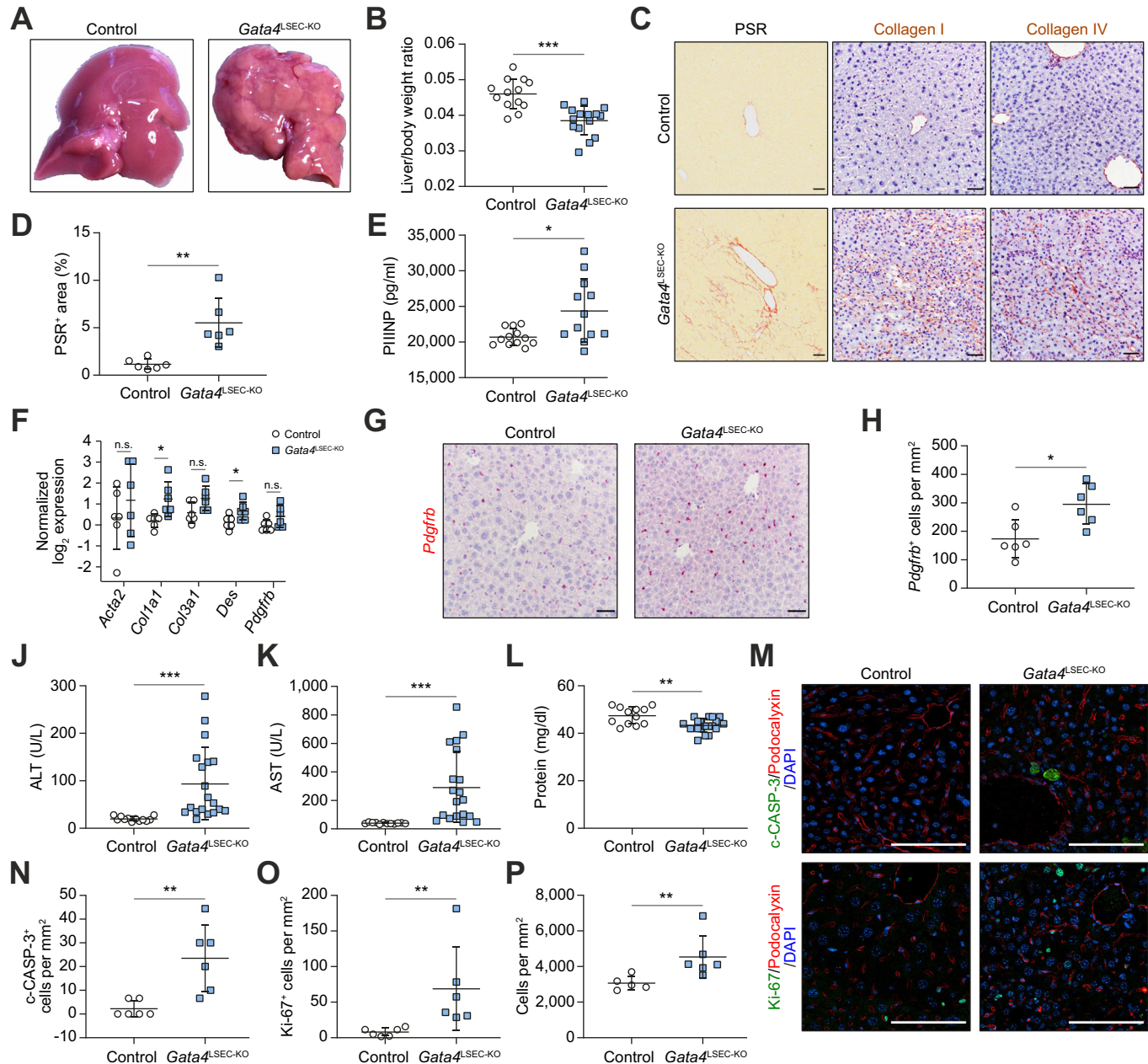


Fig. 1. Hepatic endothelial *Gata4* deficiency causes hepatopathy. (A–B) Macroscopic liver phenotype ($n = 13, 15$). (C–D) PSR staining and collagen immunohistochemistry ($n = 6$). (E) PIIINP ELISA ($n = 12$). (F) RT-qPCR for HSC activation markers ($n = 6$). (G–H) *Pdgfrb* *in situ* hybridization ($n = 6$). (J–L) Liver laboratory values ($n = 12, 19$). (M–P) Immunofluorescence of c-CASP-3, Ki-67 and cell density ($n = 6$). Scale bars: (C, G) 50 μ m; (M) 100 μ m. n.s. $p \geq 0.05$; * $p < 0.05$; ** $p < 0.01$; *** $p < 0.001$; (B, D, F, H, P) Mean \pm SD, Welch's *t* test; (E, J–L, N–O) Mean \pm SD, Mann-Whitney *U* test. HSC, hepatic stellate cell; LSEC, liver sinusoidal endothelial cell; KO, knockout; PIIINP, procollagen type III N-terminal propeptide; PSR, Picosirius red; RT-qPCR, reverse transcription quantitative PCR.

metabolic profile revealed reduction of serum glucose, cholesterol and triglycerides (Fig. S1G). Hepatopathy was accompanied by enhanced apoptosis and proliferation of hepatocytes and endothelial cells as demonstrated by significantly increased detection of cleaved Caspase-3 and Ki-67 in *Gata4*^{LSEC-KO} mice (Fig. 1M–O). Notably, there was a significant increase in DAPI cell counts (cells per mm^2 area) in *Gata4*^{LSEC-KO} livers, indicating that hepatocytes were smaller in *Gata4*^{LSEC-KO} mice (Fig. 1P).

Upon further histological analysis of *Gata4*^{LSEC-KO} livers, we observed a slightly enhanced inflammatory infiltrate consisting of CD3+ lymphocytes and CD68+ macrophages, increased numbers of mitoses and binucleated hepatocytes, as well as a significant degree of sinusoidal dilatation and focal regenerative changes of the surrounding liver tissue, while PAS, Prussian Blue and Oil Red O revealed no significant alterations (Fig. S2A–C). Likewise, a colorimetric assay did not show significant changes in hepatic triglyceride levels (Fig. S2D).

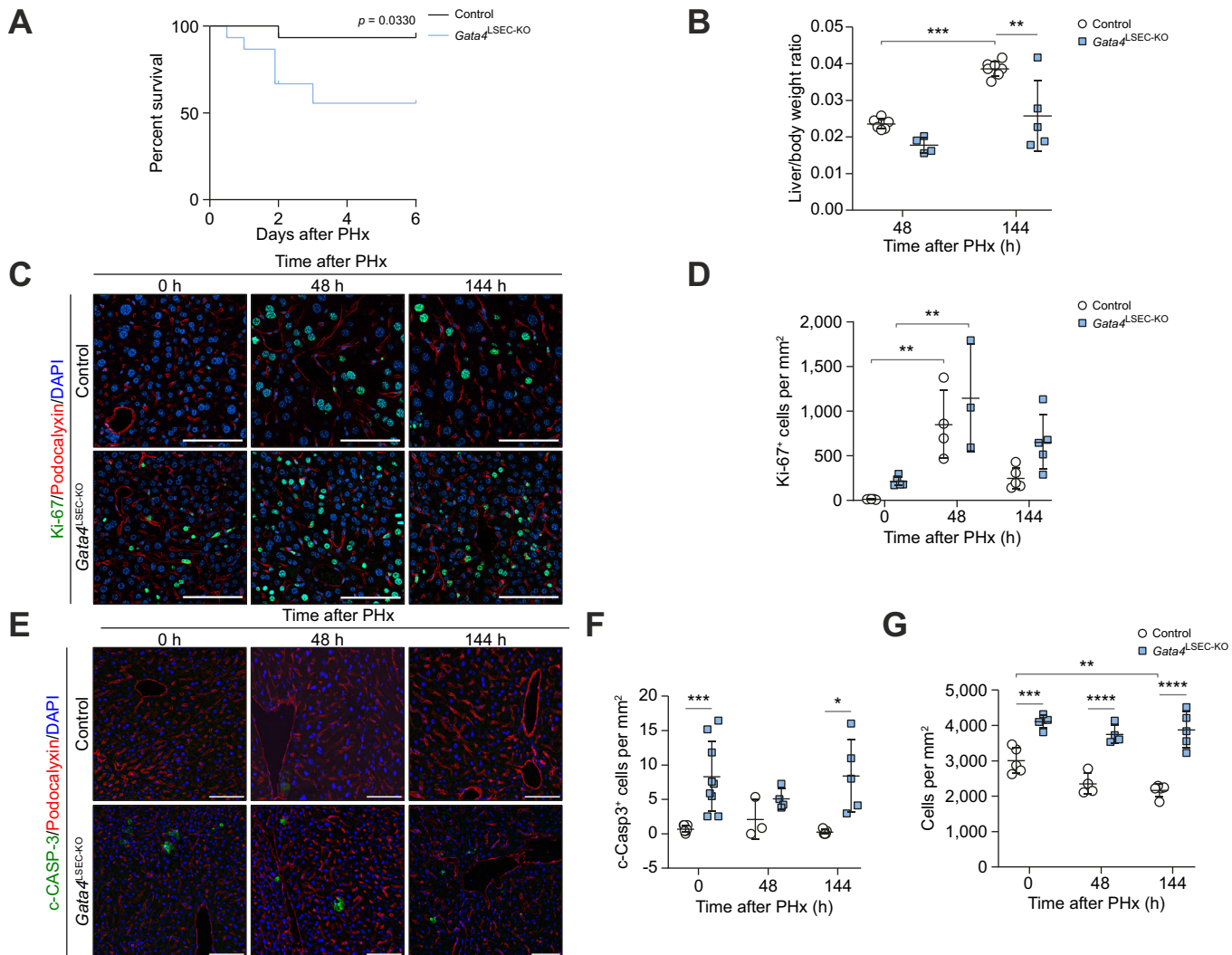


Fig. 2. Hepatic endothelial Gata4 deficiency impairs liver regeneration after PHx. (A) Kaplan–Meier curve after PHx ($n = 15$ males). (B) Liver weight to body weight ratio ($n = 4–7$). (C–D) Immunofluorescent staining for Ki-67, Podocalyxin and DAPI ($n = 4–7$). (E–F) Immunofluorescent staining for c-CASP-3, Podocalyxin and DAPI ($n = 4–7$). (G) Quantification of liver cell density in (C). Scale bars: 100 µm. * $p < 0.05$; ** $p < 0.01$; *** $p < 0.001$; **** $p < 0.0001$; (A) Log-rank test; (B, D, F, G) Mean \pm SD, two-way ANOVA with Tukey's post hoc test. LSEC, liver sinusoidal endothelial cell; KO, knockout; PHx, partial hepatectomy.

Macroscopic and histological analysis of P1, P8 and 6-week-old *Gata4*^{LSEC-KO} livers did not show major defects in liver development nor prenatal onset of liver fibrosis. While P1 livers did not have any fibrotic changes upon PSR staining, P8 and 6-week-old *Gata4*^{LSEC-KO} livers showed gradually increasing PSR values. However, these PSR values were considerably lower than the PSR values obtained from 3-month-old *Gata4*^{LSEC-KO} livers (Fig. S3A–C; Fig. 1C, D). A significant reduction in liver-to-body weight ratio was only observed in 6-week-old *Gata4*^{LSEC-KO} mice, but not in P1 or P8 mice (Fig. S3A–C).

Endothelial *Gata4* deficiency impairs liver regeneration

As hepatocyte apoptosis was accompanied by continuously elevated hepatocyte proliferation and reduced hepatocyte cell size in *Gata4*^{LSEC-KO} mice, we hypothesized that the regenerative capacity of the liver might be impaired in *Gata4*^{LSEC-KO} mice. Liver regeneration in a two-thirds partial hepatectomy model (PHx; 70%) is mediated by hepatocyte proliferation (regenerative hyperplasia, early phase/day 3–4) and by hepatocyte

enlargement (regenerative hypertrophy, later time points). After PHx, the predefined endpoints for euthanasia were reached significantly earlier in *Gata4*^{LSEC-KO} mice compared to control animals (Fig. S4A–D). All *Gata4*^{LSEC-KO} mice that did not recover after PHx failed to do so in the early phase indicating a defect in regenerative hypertrophy (Fig. 2A). In the group of the PHx *Gata4*^{LSEC-KO} mice that survived to the end of the experiment, liver-to-body weight ratio and liver weight failed to increase significantly between 48 h and 144 h after PHx in contrast to the control animals (Fig. 2B). Similarly, the liver weight had nearly doubled in the control group at 144 h after PHx, while the liver weight did not significantly increase in the *Gata4*^{LSEC-KO} mice at this late time point, indicating severe impairment rather than delay of liver regeneration (Fig. S4A).

To test for regenerative hyperplasia, we studied cell proliferation. Baseline proliferation as measured by Ki-67 positivity was already elevated in *Gata4*^{LSEC-KO} mice (Fig. 1M, O and Fig. 2C, D). Nevertheless, the numbers of proliferating cells were significantly increased after 48 h and declined after 144 h in both

Gata4^{LSEC-KO} and control mice (Fig. 2C, D) indicating that regenerative hyperplasia was not defective. Similarly, hepatocyte apoptosis was slightly, but significantly increased at baseline in *Gata4*^{LSEC-KO} mice and remained on a similar level during PHx-induced regeneration (Fig. 2E, F). To test for regenerative hypertrophy, we assessed hepatocyte size by measuring cell numbers per area. While hepatocyte size significantly increased at 48 and 144 h after PHx in control animals, this increase did not occur in *Gata4*^{LSEC-KO} mice (Fig. 2G), indicating that hepatocytes are not able to undergo regenerative hypertrophy in *Gata4*^{LSEC-KO} mice. In conclusion, regenerative hypertrophy of the liver and as a consequence liver regeneration as a whole seem to be grossly impaired in *Gata4*^{LSEC-KO} mice, while a mere delay in regeneration seems less likely.

Endothelial *Gata4* deficiency causes sinusoidal capillarization

Regarding the vasculature, hepatic microvessels in *Gata4*^{LSEC-KO} mice showed a remarkable degree of sinusoidal capillarization. Using immunofluorescent staining, ISH, or immunoblot analysis, respectively, sinusoidal endothelial cell-specific markers such as *Stab2*³ and LYVE-1 were shown to be downregulated while continuous endothelial cell-specific markers *Cd34* and Endomucin were upregulated (Fig. 3A–C). In line with loss of *Stab2* from capillarized LSECs, hyaluronic acid levels were enhanced in the peripheral blood of *Gata4*^{LSEC-KO} mice (Fig. 3D). Transmission electron microscopy showed deposition of large bundles of collagen in the space of Disse and apposition of a basement membrane beneath the capillarized LSECs (Fig. 3E). In addition, a considerable loss of hepatocyte villi was observed in the space of Disse (Fig. 3E).

Endothelial *Gata4* deficiency causes LSEC-to-continuous endothelial cell transdifferentiation

For in-depth analysis of the molecular alterations in LSECs of *Gata4*^{LSEC-KO} mice, we performed gene expression profiling of isolated LSECs. Altogether, 403 genes were significantly dysregulated in *Gata4*^{LSEC-KO} compared to control mice (Fig. 4A, Table S3). Performing overrepresentation analysis (ORA) and gene set-enrichment analysis (GSEA) with established gene sets for continuous vs. sinusoidal endothelial differentiation^{13,15,17}, we systematically confirmed that sinusoidal and continuous endothelial cell genes were suppressed or induced, respectively, indicating LSEC-to-continuous endothelial transdifferentiation in *Gata4*^{LSEC-KO} mice (Fig. 4A, B, C). Furthermore, we performed GSEA of MSigDB hallmark gene sets to identify other altered endothelial processes. Among the most regulated gene sets, we found enrichment of angiogenesis-associated genes and MYC target genes in the *Gata4*^{LSEC-KO} transcriptomic data (Fig. 4D). In another approach, ORA of the 403 significantly dysregulated genes was carried out using Enrichr. In the Gene ontology (GO) Biological Process 2018 library, ‘Extracellular matrix organization’ was identified as the most significant GO term in LSECs of *Gata4*^{LSEC-KO} mice (Fig. 4E). As GATA4 is a transcription factor (TF), we also performed ORA of the library “TF Perturbations Followed by Expression” and found GATA6 and MYC among the most strongly enriched transcription factors in LSEC of *Gata4*^{LSEC-KO} mice (Fig. 4F). Notably, MYC target genes were enriched in both GSEA and ORA approaches (Fig. 4D, F) and upregulation of MYC target genes paralleled upregulation of continuous endothelial cell genes in *Gata4*-deficient LSEC (Fig. 4C, G). Myc was also among the

significantly upregulated transcription factors in *Gata4*^{LSEC-KO} LSECs (Fig. 4H). Regarding angiocrine factors, we observed an upregulation of angiogenesis-related genes such as *Pdgfb*, *Apln* and *Vegfa* (Fig. 4J). Moreover, angiocrine factors known to control hepatocyte function, such as *Bmp2* and *Wnt2*, were significantly downregulated in *Gata4*^{LSEC-KO} LSECs (Fig. 4J).

Endothelial *Gata4* deficiency mediates a profibrotic angiocrine switch and HSC activation

To confirm the transcriptomic alterations seen in our microarray data (Fig. 5A), we performed RT-qPCR and ISH of selected genes of interest. Myc and *Pdgfb* were significantly upregulated in *Gata4*-deficient LSECs and therefore represent novel endothelial candidate genes involved in liver fibrogenesis (Fig. 5B). Angiocrine factors *Apln*, *Esm1* and *Igfbp5* were upregulated in *Gata4*-deficient LSECs, while *Bmp2* and *Wnt2* were downregulated (Fig. 5C, Fig. S5A). Analysis of extracellular matrix genes including *Sparcl1*, Collagens and Laminins further confirmed a pro-fibrotic switch in *Gata4*^{LSEC-KO} LSECs (Fig. 5D). Duplex ISH confirmed that *Pdgfb* was predominantly expressed *de novo* by endothelial cells in *Gata4*^{LSEC-KO} livers (Fig. 5E–H and Fig. S5B, C). Likewise, endothelial Myc was significantly upregulated in *Gata4*^{LSEC-KO} livers (Fig. 5J, Fig. S5A). *Sparcl1* was expressed *de novo* by both endothelial cells and HSCs in *Gata4*^{LSEC-KO} livers (Fig. S5D, E). In line with the higher number of *Pdgfrb*-expressing HSCs (Fig. 1G, H), *Col1a1* was expressed mainly by HSCs, indicating HSC activation (Fig. S5F).

Increased chromatin accessibility and amplification by activated MYC mediate *de novo* endothelial *Pdgfb* expression

To investigate how endothelial *Gata4* deficiency leads to activation of the transcription factor MYC and its downstream targets, we performed genome-wide analysis of open chromatin landscapes using ATAC-seq of LSECs isolated from *Gata4*^{LSEC-KO} and control mice. Importantly, we found that GATA4 controls gene expression by regulating chromatin accessibility. ATAC-seq revealed increased chromatin accessibility at a multitude of gene loci in *Gata4*^{LSEC-KO} LSECs, including the *Myc* and the *Pdgfb* gene loci that were directly bound by GATA4 (Fig. 5K, L).

In a more global approach, we intersected the gene expression profiling data and ATAC-seq data obtained from *Gata4*^{LSEC-KO} LSECs and found that chromatin accessibility was highly increased for the genes significantly upregulated in *Gata4*^{LSEC-KO} LSECs (Fig. 5M). Conversely, no changes in chromatin accessibility were found for genes significantly downregulated in *Gata4*^{LSEC-KO} LSECs (Fig. 5M). These results indicate that the repressive function of GATA4 is executed on the chromatin level, whereas its activating function is independent of alterations in chromatin accessibility.

Notably, we identified MYC binding sites at the promotor region of the *Pdgfb* gene using the ATAC-seq peaks differentially regulated in *Gata4*-deficient LSECs combined with the published MYC-ChIP-seq data of the liver¹⁸ (Fig. 5L). To further study the binding of the transcription factor MYC at the promoter region of the angiocrine factor *Pdgfb*, we performed MYC ChIP-qPCR. MYC binding at *Pdgfb* was increased in LSECs from *Gata4*^{LSEC-KO} mice compared to control mice in 3 biologically independent ChIP experiments. These results suggest that MYC directly augments *Pdgfb* expression in *Gata4*^{LSEC-KO} LSECs (Fig. 5N).

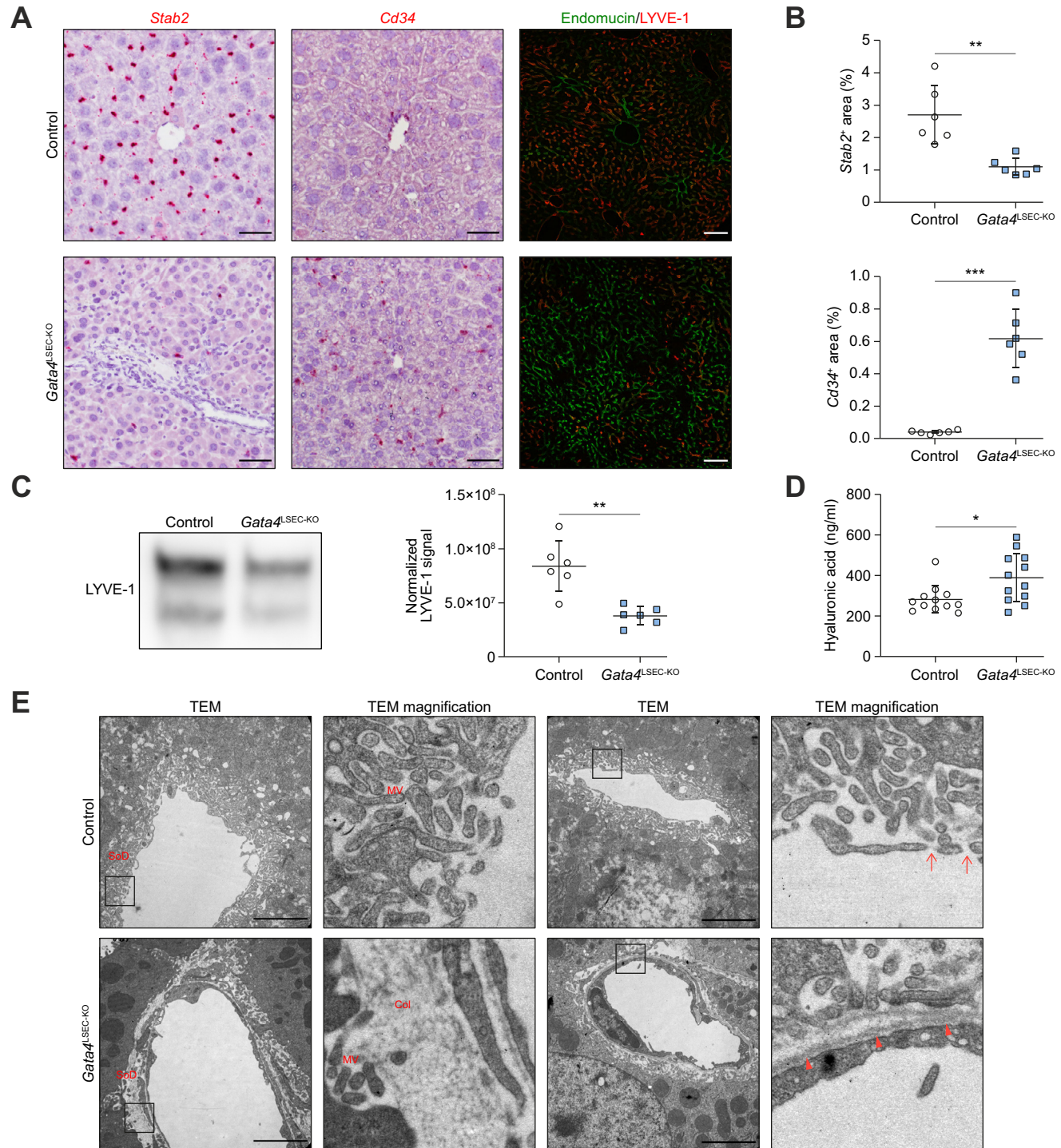


Fig. 3. Hepatic endothelial Gata4 deficiency causes sinusoidal capillarization. (A–B) *In situ* hybridization for *Stab2*, *Cd34*, and immunofluorescent staining for Endomucin and LYVE-1 (n = 6). Scale bars: *in situ* hybridization 50 µm; immunofluorescence 100 µm. (C) Western Blot of LYVE-1 in LSECs (n = 6). (D) Hyaluronic acid in plasma (n = 12). (E) TEM of livers (n = 2–3 males). Red arrowheads: basement membrane. Red arrows: endothelial fenestrae. Scale bars: 3 µm. *p < 0.05; **p < 0.01; ***p < 0.001; Mean ± SD; (B–C) Welch's t test; (D) Mann-Whitney U test. Col, collagen; LSEC, liver sinusoidal endothelial cell; KO, knockout; MV, microvilli; SoD, space of Disse.

Endothelial Gata4 deficiency causes downregulation of angiocrine Wnt signaling, impairing metabolic liver zonation and liver regeneration

Furthermore, we confirmed the regulation of other angiocrine factors targeting hepatocytes in endothelial Gata4-deficiency.

Wnt2 was downregulated in Gata4-deficient LSECs (Fig. S6A), whereas *Wnt9b*, *Rspo3* and *Hgf* were slightly increased or unchanged (Fig. S6A–C). As a consequence, angiocrine-mediated β-catenin signaling was impaired in hepatocytes, as demonstrated by reduced hepatocyte *Axin2* expression

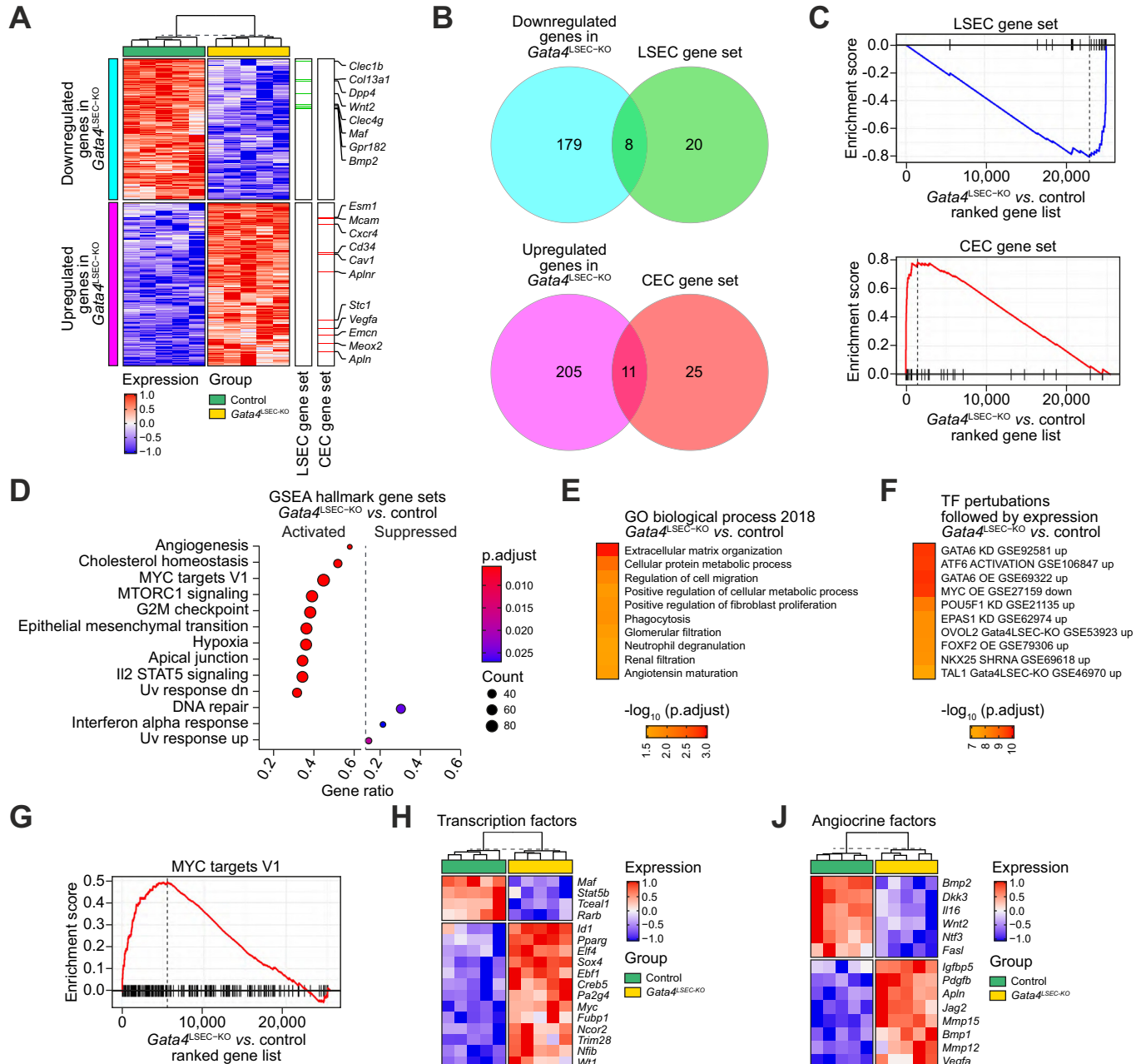


Fig. 4. Hepatic endothelial *Gata4* deficiency causes molecular transdifferentiation of LSECs comprising a profibrotic angiocrine switch. (A–B) Significant genes ($P_{adj} < 0.05$) and annotation for LSEC ($p = 0.0200$) and CEC ($p = 0.0011$) gene sets. (C) Enrichment plots of LSEC-associated ($p = 0.0018$, NES = -2.58) and CEC-associated ($p = 0.0021$, NES = 2.65) genes ($n = 5$). (D) GSEA using MSigDB hallmark gene sets. (E–F) ORA of selected gene ontology and transcription factor libraries. (G) Enrichment plot of MYC target genes ($P_{adj} = 0.0005$, NES = 2.24). Heat maps of (H) transcription and (J) angiocrine factors. (A) Fisher's exact test. CEC, continuous endothelial cell; LSEC, liver sinusoidal endothelial cell; KO, knockout; GSEA, gene set-enrichment analysis; NES, normalized enrichment score; ORA, overrepresentation analysis.

(Fig. S6A). Consequently, metabolic liver zonation was disturbed as shown by reduced glutamine synthetase expression in *Gata4*^{LSEC-KO} mice (Fig. S6A). To further corroborate these results, we performed gene expression analysis of whole livers from *Gata4*^{LSEC-KO} mice vs. control animals. GSEA of *Gata4*^{LSEC-KO} livers showed that major metabolic pathways were affected, including fatty acid metabolism, bile acid metabolism, oxidative phosphorylation and xenobiotic metabolism (Fig. S6D).

As angiocrine factors Wnt-2 and HGF are known to contribute to liver regeneration,¹⁹ we analyzed these factors in *Gata4*^{LSEC-KO} mice after PHx. After an initial increase of *Hgf* in both, *Gata4*^{LSEC-KO} and control LSEC, *Hgf* remained elevated only in *Gata4*^{LSEC-KO} LSECs at 144 h after PHx, indicating that regeneration was not successful despite *Hgf* induction and hepatocyte proliferation, i.e. regenerative hyperplasia (Fig. S7A). In contrast to control animals, angiocrine *Wnt2* expression did not increase in *Gata4*^{LSEC-KO} LSECs at 48 h after PHx (Fig. S7B). As induction of angiocrine Wnt-2 signaling is

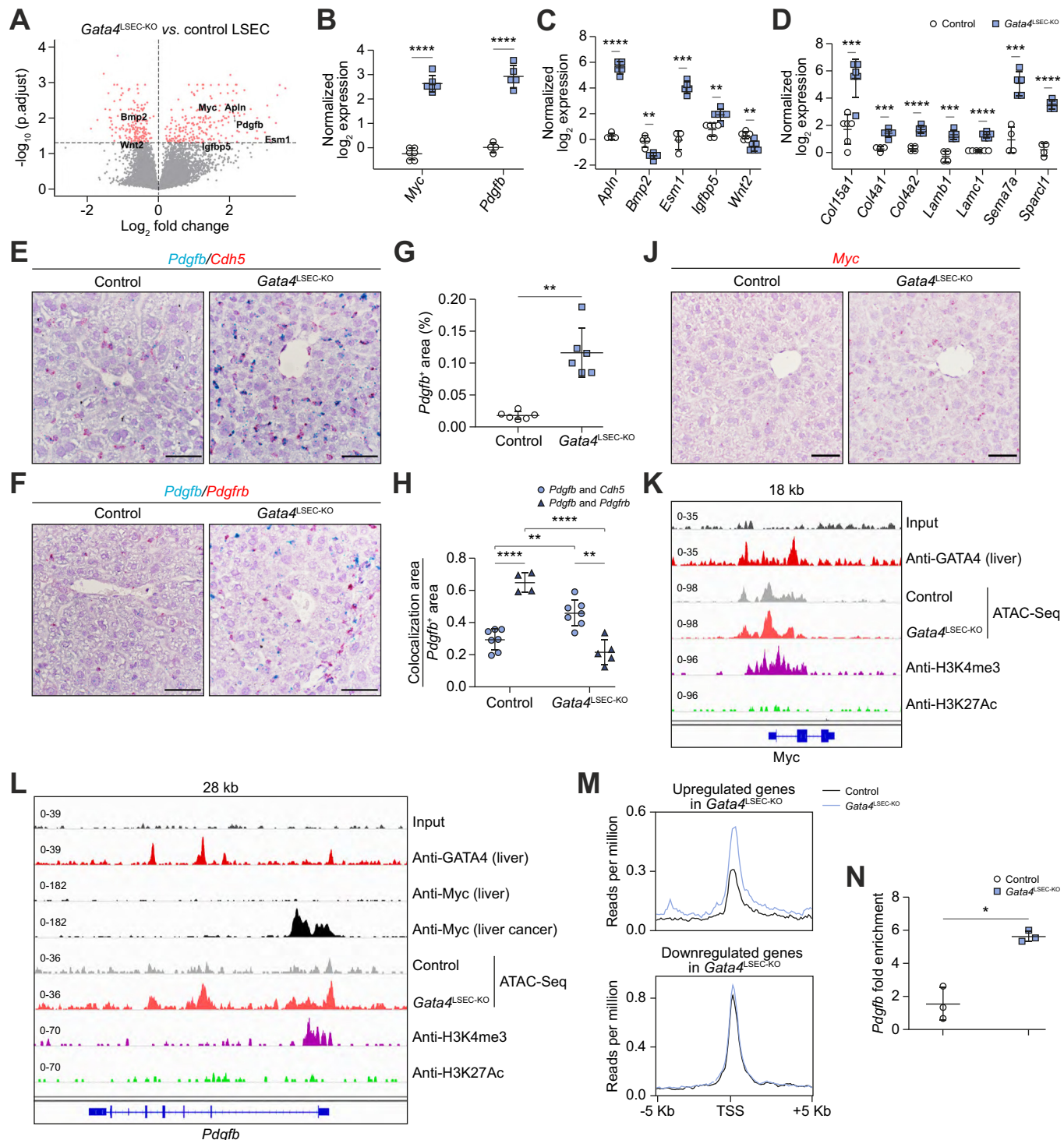


Fig. 5. Angiocrine PDGFB signaling in Gata4^{LSEC-KO} mice mediates stellate cell activation. (A) Volcano plot of LSEC transcriptomic data (n = 5 males). (B–D) RT-qPCR of LSEC for selected genes (n = 5 males). (E–H) *In situ* hybridization of liver tissue for *Pdgfb* with *Cdh5* or *Pdgfrb* (n = 6 females). (J) *Myc* *In situ* hybridization of livers. (K–L) Genome tracks of GATA4-ChIP-Seq, MYC-ChIP-Seq (L), histone marker-ChIP-seq, and ATAC-Seq on the *Myc* and *Pdgfb* loci. (M) ATAC-Seq reads mapped around transcription-start-sites of upregulated and downregulated genes in *Gata4*^{LSEC-KO}. (N) ChIP-qPCR to analyze MYC occupancy at *Pdgfb* promoter in LSECs (n = 3); Scale bars: 50 µm. *p < 0.05; **p < 0.01; ***p < 0.001; ****p < 0.0001; (B–D, G, N) Mean ± SD; Welch's t test; (H) Mean ± SD; two-way ANOVA with Tukey's post hoc test. ATAC-seq, assay for transposase-accessible chromatin using sequencing; ChIP-seq, chromatin immunoprecipitation sequencing; KO, knockout; LSEC, liver sinusoidal endothelial cell; RT-qPCR, reverse transcription PCR.

a hallmark of the early phase of liver regeneration, impaired induction of *Wnt2* in *Gata4^{LSEC-KO}* mice likely contributes to

insufficient regeneration in these animals by impairing regenerative hypertrophy.

Endothelial GATA4 protects against CDAA diet-associated perisinusoidal liver fibrogenesis

As the liver fibrosis seen in *Gata4*^{LSEC-KO} mice resembles the perisinusoidal fibrosis of non-alcoholic steatohepatitis, we studied the hepatic endothelium in choline-deficient, l-amino acid-defined (CDAA) diet-induced liver fibrosis.

In CDAA diet-fed mice, perisinusoidal liver fibrosis developed after 10 weeks (Fig. 6A, B) accompanied by development of hepatic steatosis and moderate hepatopathy (Fig. S8A, B). RT-qPCR analysis of whole liver specimens demonstrated activation of HSCs (Fig. 6C). Gene expression profiling of LSECs isolated from CDAA diet-fed mice (CDAA LSECs) showed similar downregulation of LSEC-specific genes (Fig. 6D–F) as seen in LSECs of *Gata4*^{LSEC-KO} mice (Fig. 4A–C). Similarly, GSEA of CDAA LSECs revealed results partially overlapping with those found in *Gata4*^{LSEC-KO} LSECs, identifying MYC target genes as the top enriched gene set (Fig. 6G). ORA of 3,890 significantly dysregulated genes revealed 'Cell migration' and 'Extracellular matrix organization' as the most strongly enriched gene sets (Fig. 6H). We also performed ORA of the library "TF Perturbations Followed by Expression" and found SOX9 and GATA6 gene sets to be the most significantly regulated gene sets (Fig. 6J). Comparing microarray data from *Gata4*^{LSEC-KO} and CDAA LSECs revealed a remarkable overlap of up- and downregulated genes (Fig. 6K, L). Accordingly, many transcription and angiocrine factors were regulated in the same direction including *Myc* and *Pdgfb* (Fig. 6M, N). These results demonstrate congruent alterations in the endothelial transcriptomic profile of *Gata4*^{LSEC-KO} LSECs and CDAA LSECs compared to control animals or standard-fed mice, respectively.

To investigate whether endothelial GATA4 function is affected in CDAA-fed mice, we defined a GATA4 gene set as an indicator for GATA4 function. To this end, we combined transcriptional and regulatory data from 3 different sources (Fig. 7A): (i) significantly downregulated genes from *Gata4*^{LSEC-KO} LSECs from this study, and ChIP-seq data for GATA4 of whole liver from (ii) ENCODE (ENCSR194GNY) and (iii) GEO (GSM1194141). 73 genes were identified that were significantly downregulated in *Gata4*^{LSEC-KO} LSECs and exhibited ≥2 binding sites for GATA4 in either or both ChIP-seq data sets (Table S4). The gene set of these 73 genes was regarded as a reporter for GATA4 activity and named "Endothelial GATA4 gene set". Using the "Endothelial GATA4 gene set" for GSEA on endothelial cells from CDAA-fed mice, we found enrichment for the gene set in LSECs of standard-fed mice indicating a reduction of GATA4-dependent genes in the CDAA model of liver fibrosis (Fig. 7B, C). On the contrary, MYC target genes were enriched in endothelial cells from CDAA-fed mice (Fig. 7D). These findings imply antagonistic functions of endothelial GATA4 and MYC in liver fibrogenesis. Confirming the results regarding the regulation of the GATA4 and MYC target gene sets in CDAA LSECs, *Gata4* and *Myc* themselves were differentially expressed in CDAA LSECs and LSECs from standard-fed control animals, respectively. While GATA4 was significantly downregulated (Fig. 7E, F), *Myc* and *Pdgfb* were significantly upregulated (Fig. 7E).

Based on the findings that acquired endothelial GATA4 downregulation may contribute to CDAA-associated perisinusoidal liver fibrosis, we asked whether complete genetic endothelial *Gata4* deficiency further aggravates CDAA-induced liver fibrogenesis. When *Gata4*^{LSEC-KO} mice were fed the CDAA diet (Fig. S9A), the amount of perisinusoidal liver fibrosis was

significantly increased compared to both CDAA-fed control mice and standard-fed *Gata4*^{LSEC-KO} mice (Fig. 7G, H). While hepatopathy was not greatly different in CDAA-fed control and *Gata4*^{LSEC-KO} mice (Fig. 7J, K), HSC activity as measured by expression of extracellular matrix molecules *Acta2*, *Col1a1* and *Col3a1* was significantly higher in CDAA-fed *Gata4*^{LSEC-KO} mice compared to both CDAA-fed control mice and standard-fed *Gata4*^{LSEC-KO} mice (Fig. 7L). In contrast to the aggravation of perisinusoidal liver fibrosis in CDAA-fed *Gata4*^{LSEC-KO} mice, no significant changes in the extent of bridging fibrosis were seen in *Gata4*^{LSEC-KO} mice upon induction of toxic liver fibrosis in the carbon tetrachloride model (Fig. S9C–F).

In conclusion, downregulation of GATA4 and its downstream target genes seems to be an important pathogenic factor in the development of CDAA-associated perisinusoidal fibrosis. Although there might be additional mechanisms that add to the complex phenotype in CDAA-fed mice, our results show that endothelial GATA4 protects against dietary perisinusoidal liver fibrosis.

Analysis of single cell RNA-seq data reveals that the endothelial GATA4/PDGFB axis is also affected in human cirrhosis

To validate our results, we analyzed a published single cell transcriptome sequencing (scRNA-seq) dataset of human liver non-parenchymal cells including endothelial cells from patients with cirrhosis and healthy control individuals.²⁰ Louvain clustering yielded 33 different cell clusters from which endothelial cells were identified by the expression of *PECAM1*, *CDH5* and the endothelial transcription factor *ERG* (Fig. 8A–E).

Endothelial cells with expression of markers *GATA4* and *STAB2* or *GATA4* and *WNT2* were defined as LSECs. While the cluster of endothelial cells from healthy livers mainly consisted of LSECs, endothelial cells from cirrhotic livers were mainly non-LSEC endothelial cells (Fig. 8F–J). These results demonstrate that endothelial cells from cirrhotic patients have undergone a transdifferentiation process with loss of *STAB2* and *GATA4* expression (Fig. 8K, L). Notably, *PDGFB* was induced in the endothelial cells of cirrhotic patients (Fig. 8M).

We performed GSEA using the MSigDB hallmark gene sets and compared LSEC vs. non-LSEC endothelial cell data. "MYC targets" and "Angiogenesis" were the top 2 enriched gene sets in non-LSEC endothelial cells (Fig. S10A, B). Meanwhile, the endothelial GATA4 gene set defined in this study was enriched in LSECs (Fig. S10C).

In conclusion, these data support the notion of a remarkable congruence between murine and human endothelial cell alterations during liver fibrosis/cirrhosis. This indicates that the antagonistic counterplay of endothelial GATA4 and MYC represents a common pathway contributing to liver fibrogenesis in mice and humans.

Discussion

Our data show that compromising LSEC differentiation leads to hepatopathy, sinusoidal capillarization, and perisinusoidal liver fibrosis. Protection against liver fibrosis is mediated by endothelial expression of the sinusoidal master regulator GATA4. Loss of GATA4 expression in LSECs is permissive for induction of the sinusoidal capillarization program and allows *de novo* expression of profibrotic angiocrine factors including *Pdgfb*, *Sparc1*, *Esm1* and *Igfbp5*.

Notably, the regulation of MYC and GATA4 was antagonistic. As a consequence, endothelial GATA4 and MYC target gene sets

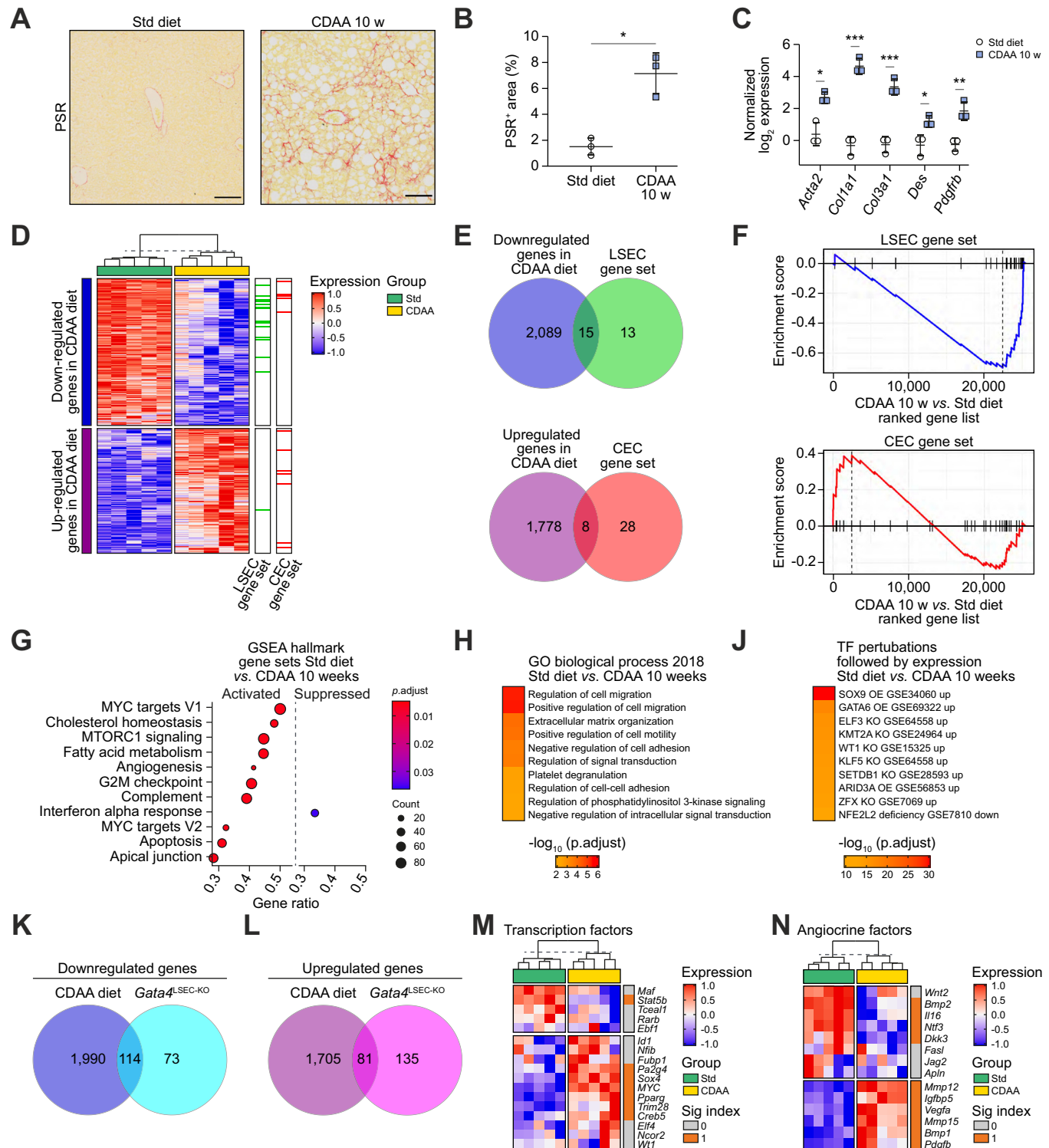


Fig. 6. Diet-induced perisinusoidal liver fibrosis recapitulates loss of GATA4 and the angiocrine switch. (A–B) PSR staining of livers. Scale bars: 100 µm. (n = 3). (C) RT-qPCR for HSC activation markers (n = 3). (D–E) Significant genes ($P_{adj} < 0.05$) and annotation for LSEC ($p = 0.0015$) and CEC ($p = 0.2787$) gene sets. (F) Enrichment plot of LSEC-associated ($p = 0.0019$, NES = -2.11) and CEC-associated ($p = 0.15$, NES = 1.27) genes. (G) GSEA using the MSigDB hallmark gene sets. (H–J) ORA of selected gene ontology and transcription factor libraries. (K–L) Overlap between genes in *Gata4^{LSEC-KO}* and CDAA diet. Heat maps of (M) transcription and (N) angiocrine factors significantly regulated in *Gata4^{LSEC-KO}* with annotation for their expression and significance upon CDAA diet. * $p < 0.05$; ** $p < 0.01$; *** $p < 0.001$; (B–C) Welch's t test. (D) Fisher's exact test. CDAA, choline-deficient, l-amino acid-defined; CEC, continuous endothelial cell; GSEA, gene set-enrichment analysis; HSC, hepatic stellate cell; LSEC, liver sinusoidal endothelial cell; KO, knockout; NES, normalized enrichment score; ORA, overrepresentation analysis; PSR, Picosirius red; RT-qPCR, reverse transcription PCR.

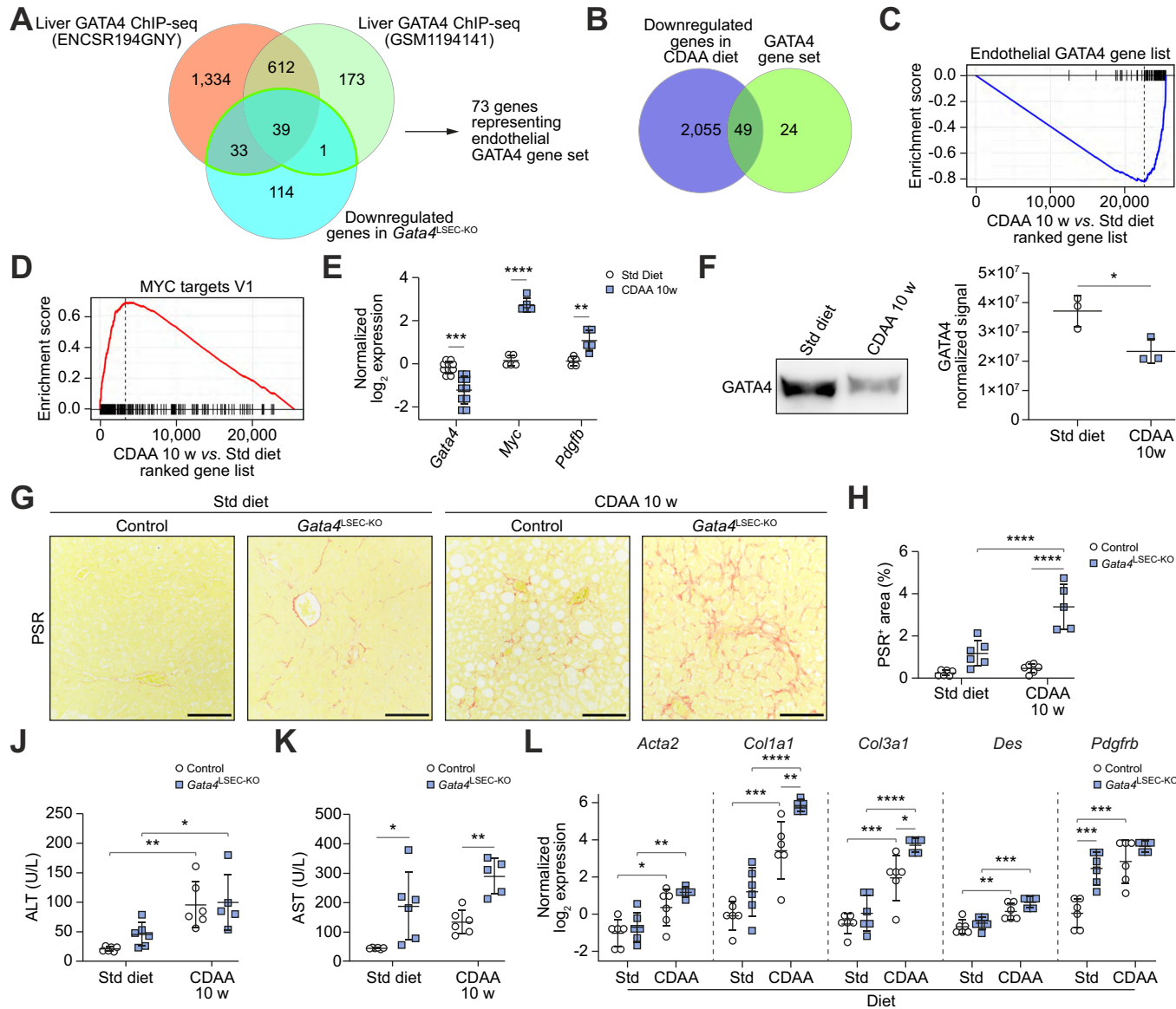


Fig. 7. Endothelial GATA4 serves as protective factor preventing perisinusoidal liver fibrosis in CDAA diet. (A) Approach to defining the endothelial *Gata4*-gene-set. (B) Overlap of downregulated genes upon CDAA diet and endothelial *Gata4*-gene-set. (C) Enrichment plot of endothelial *Gata4*-gene-set ($p = 0.0018$, $NES = -3.08$), and (D) MYC target genes ($Padj = 0.0007$, $NES = 1.98$) in LSEC. (E) RT-qPCR analysis of LSEC ($n = 5$). (F) Immunoblot for GATA4 of whole liver ($n = 3$). (G–H) PSR staining of liver ($n = 5$ –6>). Scale bars: 100 μ m. (J–K) Liver laboratory values. (L) RT-qPCR for HSC activation markers ($n = 5$ –6>). (E–F, H–L) Mean \pm SD; * $p < 0.05$; ** $p < 0.01$; *** $p < 0.001$; **** $p < 0.0001$; (E–F) Welch's t test; (H–L) two-way ANOVA with Tukey's post-hoc test. CDAA, choline-deficient, l-amino acid-defined; HSC, hepatic stellate cell; LSEC, liver sinusoidal endothelial cell; KO, knockout; NES, normalized enrichment score; PSR, Picrossirius red; RT-qPCR, reverse transcription PCR.

were also counter-regulated and this was further paralleled by counter-regulation of LSEC genes and continuous endothelial cell genes at large. Preferentially, MYC is not an on-off specifier of gene activity, but is a non-linear amplifier of expression, acting universally at active genes.²¹ By performing ATAC-seq of LSECs from *Gata4*^{LSEC-KO} and control mice, we demonstrate here that GATA4 deficiency in LSECs leads to de-repression of a general (continuous) endothelial cell differentiation program mediated by increased chromatin accessibility. Improved chromatin accessibility may then allow activation of the respective genes by MYC for which chromatin accessibility and expression are also increased upon *Gata4* depletion in LSECs. Interestingly, the

significant enrichment of MYC at the *Pdgfb* promoter region in *Gata4*^{LSEC-KO} LSECs indicates a GATA4- and MYC-dependent activation of *Pdgfb* in our model. Notably, *Pdgfb* is expressed in the microvasculature of most organs except the liver, making it a constitutive angiokine of continuous endothelial cells. This is in line with the results from ATAC-seq which suggested that GATA4 acts as a repressor of *Pdgfb* and other continuous endothelial cell genes in LSECs. Functionally, angiocrine PDGFB signaling is indispensable for pericyte maintenance,²² a cell type not found in the liver sinusoids.

De novo expression of angiocrine *Pdgfb* in LSECs alone seems to be sufficient to induce perisinusoidal fibrosis, as has been

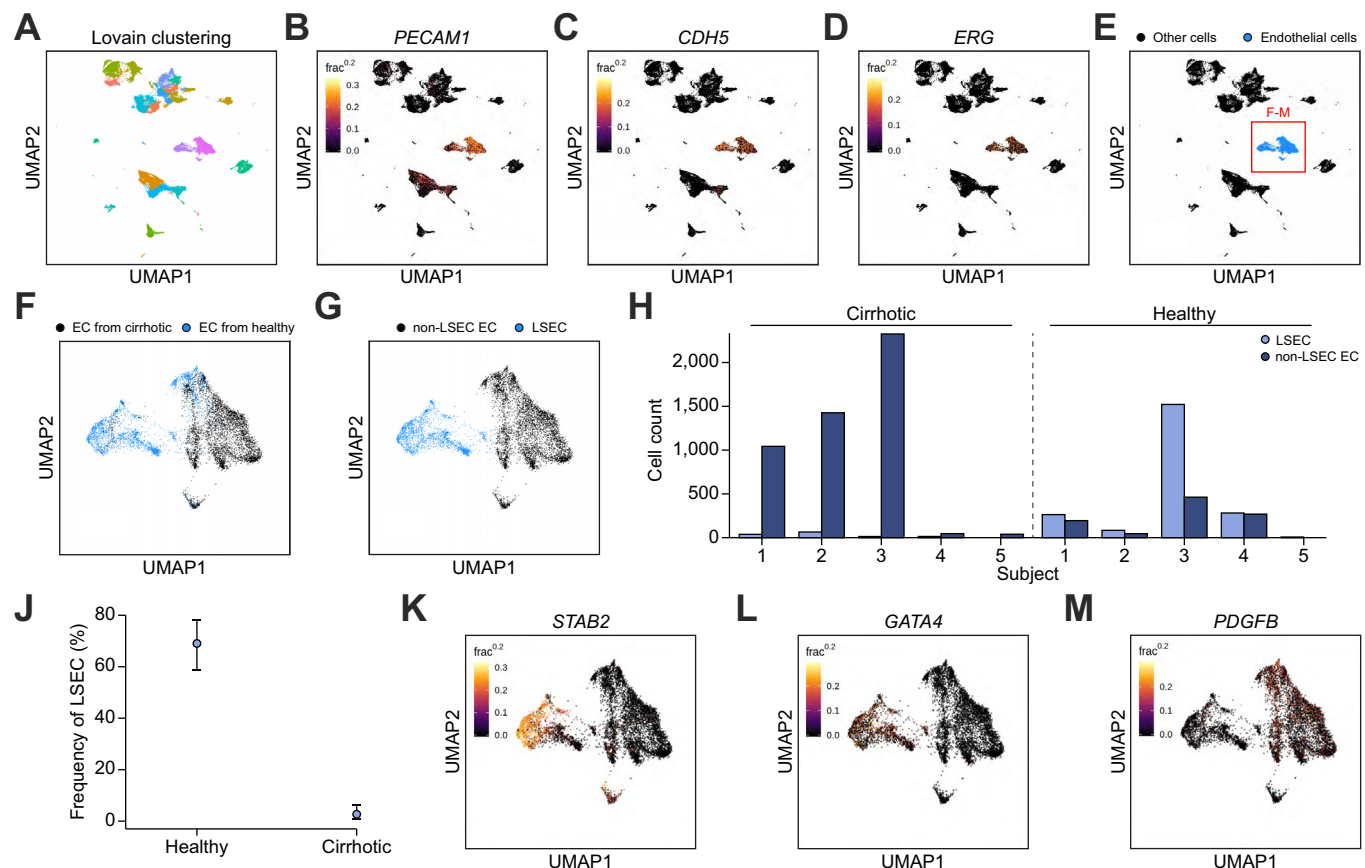


Fig. 8. Single cell transcriptome sequencing in human liver fibrosis reveals that the endothelial GATA4/PDGFB axis is affected. (A) Louvain clustering of 66,135 non-parenchymal cells from liver cirrhosis patients and healthy individuals ($n = 5$). Scaled gene expression of endothelial genes (B) *PECAM1*, (C) *CDH5* and (D) *ERG*. (E) Annotation of endothelial cells in blue. Annotation of endothelial cells by (F) condition and (G) EC subtype. (H) Count of non-LSEC EC and LSEC. (J) Frequency of LSEC in livers ($n = 5$). Error bars: 95% CI. Scaled expression of (K) *STAB2*, (L) *GATA4* and (M) *PDGFB*. EC, endothelial cell; LSEC, liver sinusoidal endothelial cell.

demonstrated by artificial *Pdgfb* overexpression in hepatocytes.²³ Vice versa, loss of *Pdgfb* activity increases hepatic permeability, prevents sinusoidal capillarization, and improves insulin sensitivity²⁴ indicating the importance of balanced PDGFB signaling for the homeostasis of the hepatic vascular niche.

Notably, endothelial *Gata4* deficiency caused non-fatal, peri-sinusoidal liver fibrosis, but not progressive periportal or bridging-type liver fibrosis in *Gata4*^{LSEC-KO} mice. This may be due to the fact that only CD248⁺ HSCs, that are induced by hepatocyte damage, are permissive for overall activation by PDGFB comprising proliferation and migration.²⁵ Furthermore, a recent study using single cell RNA-seq shows that HSCs are zonated along the liver sinusoids from pericentral to periportal²⁶; central vein-associated HSCs were identified as the major HSC subpopulation driving liver fibrosis. This differential reactivity of HSCs was also confirmed in a recent study demonstrating that loss of hepatocyte-derived ECM-1 induced moderate perisinusoidal, but massive pericentral liver fibrosis.²⁷ Therefore, additional hits may be necessary to allow angiocrine PDGFB to exert its full profibrotic effects and to finally mediate progressive portal and bridging fibrosis.²⁸

Regarding the other members of the profibrotic angiocrine panel identified in LSECs of *Gata4*^{LSEC-KO} mice, SPARCL1 may interact with PDGFB-activated HSCs to enhance collagen I fibril

formation.²⁹ Interestingly, *Sparcl1* is also induced in HSCs in non-alcoholic steatohepatitis (NASH), but not toxic liver fibrosis.³⁰ *Esm1* and *Igfbp5* were also significantly regulated angiocrine factors in LSECs of *Gata4*^{LSEC-KO} mice and they are known biomarkers for liver fibrosis.^{31,32}

Perisinusoidal liver fibrosis is a special feature in the early stage of NASH which is caused by a cascade of pathogenic hits that lead to hepatocyte and non-parenchymal liver cell damage. Although data have been grossly lacking, LSECs have been suggested to play a pivotal role among the non-parenchymal cells of the hepatic vascular niche in NASH.³³ Notably, in-depth analysis of the single cell RNA-seq data of human cirrhotic liver specimens published by Ramachandran and colleagues²⁰ regarding LSEC differentiation has largely confirmed our experimental findings in *Gata4*^{LSEC-KO} mice and CDA-induced, dietary liver fibrosis. Therefore, our data provide proof of principle that dysregulation of antagonistically acting endothelial transcriptional regulators GATA4 and MYC leads to downstream disturbance of the PDGFB/PDGFR β axis and contributes to murine and human liver fibrosis.

In conclusion, we have shown here that liver endothelial cells actively drive and determine perisinusoidal liver fibrogenesis, with the transcription factor GATA4 acting as the master regulator of chromatin accessibility. Therefore, therapies targeting

the GATA4/MYC/PDGFB/PDGFR β axis represent a promising strategy for the prevention and treatment of liver fibrosis.³⁴

Abbreviations

ATAC-seq, assay for transposase-accessible chromatin using sequencing; CDAA, choline-deficient, l-amino acid-defined; ChIP-seq, chromatin immunoprecipitation sequencing; GSEA, gene set-enrichment analysis; HSC, hepatic stellate cell; ISH, *in situ* hybridization; KO, knockout; LSEC, liver sinusoidal endothelial cell; MSigDB, molecular signatures database; NES, normalized enrichment score; ORA, overrepresentation analysis; PHx, partial hepatectomy; PIIINP, procollagen type III N-terminal propeptide; PSR, Picrosirius red; RT-qPCR, reverse transcription quantitative PCR.

Financial support

The authors gratefully acknowledge the data storage service SDS@hd supported by the Ministry of Science, Research and the Arts Baden-Württemberg (MWK) and the German Research Foundation (DFG) through grant INST 35/1314-1 FUGG and INST 35/1503-1 FUGG. This work was supported by the Deutsche Forschungsgemeinschaft, Germany (DFG, German Research Foundation) – Project numbers 259332240 – RTG/GRK 2099; 394046768 – CRC/SFB 1366; 314905040 – CRC/SFB-TR 209; 413262200 – ICON/EB 187/8-1.

Conflict of interest

The authors declare no competing interests.

Please refer to the accompanying ICMJE disclosure forms for further details.

Authors' contributions

Conceptualization, M.W., T.S., S.W.K., C.G., P.-S.K., S.G.; Investigation, M.W., T.S., S.W.K., C.D.S., H.S., J.C., L.K., A.M., C.S., M.N., X.-J.Z.; Data Curation, M.W., C.D.S., J.C., C.S., G.D.; Writing – Original Draft, C.G., P.-S.K., S.G.; Writing – Review & Editing, M.W., T.S., S.W.K., C.D.S., H.S., J.C., L.K., A.M., C.S., M.N., A.U., S.A., X.-J.Z., G.v.F., D.H., C.M., G.D., K.S., C.G., P.-S.K., S.G.; Visualization, M.W., T.S., S.W.K., C.D.S., A.U., K.S.; Supervision, C.G., P.-S.K., S.G.; Funding Acquisition, M.W., S.A., C.M., G.D., C.G., P.-S.K., S.G.

Data availability statement

The raw and normalized gene expression profiling data have been deposited in NCBI's Gene Expression Omnibus and are accessible through GEO Series accession number GSE141004 (<https://www.ncbi.nlm.nih.gov/geo/query/acc.cgi?acc=GSE141004>). ATAC ('assay for transposase-accessible chromatin')-sequencing (ATAC-seq) and chromatin immunoprecipitation (ChIP)-sequencing (ChIP-seq) data are accessible through accession number GSE154828 (<https://www.ncbi.nlm.nih.gov/geo/query/acc.cgi?acc=GSE154828>).

Acknowledgments

We thank Stephanie Riester and Carolina De La Torre for excellent technical support.

Supplementary data

Supplementary data to this article can be found online at <https://doi.org/10.1016/j.jhep.2020.08.033>.

References

Author names in bold designate shared co-first authorship

- [1] Augustin HG, Koh GY. Organotypic vasculature: from descriptive heterogeneity to functional pathophysiology. *Science* 2017;357:eaa12379.
- [2] Shetty S, Lalor PF, Adams DH. Liver sinusoidal endothelial cells - gatekeepers of hepatic immunity. *Nat Rev Gastroenterol Hepatol* 2018;15:555–567.
- [3] Schledzewski K, Géraud C, Arnold B, Wang S, Gröne H-J, Kempf T, et al. Deficiency of liver sinusoidal scavenger receptors stabilin-1 and -2 in mice causes glomerulofibrotic nephropathy via impaired hepatic clearance of noxious blood factors. *J Clin Invest* 2011;121:703–714.
- [4] Halpern KB, Shenhar R, Massalha H, Toth B, Egozi A, Massasa EE, et al. Paired-cell sequencing enables spatial gene expression mapping of liver endothelial cells. *Nat Biotechnol* 2018;36:962–970.
- [5] Rafii S, Butler JM, Ding B-S. Angiocrine functions of organ-specific endothelial cells. *Nature* 2016;529:316–325.
- [6] Koch P-S, Olsavszky V, Ulbrich F, Sticht C, Demory A, Leibing T, et al. Angiocrine Bmp2 signaling in murine liver controls normal iron homeostasis. *Blood* 2017;129:415–419.
- [7] Leibing T, Géraud C, Augustin I, Boutros M, Augustin HG, Okun JG, et al. Angiocrine Wnt signaling controls liver growth and metabolic maturation in mice. *Hepatology* 2018;68:707–722.
- [8] Wang B, Zhao L, Fish M, Logan CY, Nusse R. Self-renewing diploid Axin2(+) cells fuel homeostatic renewal of the liver. *Nature* 2015;524:180–185.
- [9] Ding B-S, Cao Z, Lis R, Nolan DJ, Guo P, Simons M, et al. Divergent angiocrine signals from vascular niche balance liver regeneration and fibrosis. *Nature* 2014;505:97–102.
- [10] Xie G, Wang X, Wang L, Wang L, Atkinson RD, Kanel GC, et al. Role of differentiation of liver sinusoidal endothelial cells in progression and regression of hepatic fibrosis in rats. *Gastroenterology* 2012;142:918–927.e6.
- [11] Maretti-Mira AC, Wang X, Wang L, DeLeve LD. Incomplete differentiation of engrafted bone marrow endothelial progenitor cells initiates hepatic fibrosis in the rat. *Hepatology* 2019;69:1259–1272.
- [12] Desroches-Castan A, Tillet E, Ricard N, Ouarné M, Mallet C, Belmudes L, et al. Bone morphogenetic protein 9 is a paracrine factor controlling liver sinusoidal endothelial cell fenestration and protecting against hepatic fibrosis. *Hepatology* 2019;70:1392–1408.
- [13] Wohlfel SA, Häfele V, Dietsch B, Schledzewski K, Winkler M, Zierow J, et al. Hepatic endothelial notch activation protects against liver metastasis by regulating endothelial-tumor cell adhesion independent of angiocrine signaling. *Cancer Res* 2019;79:598–610.
- [14] Dufton NP, Peghaire CR, Osuna-Almagro L, Raimondi C, Kalna V, Chauhan A, et al. Dynamic regulation of canonical TGF β signalling by endothelial transcription factor ERG protects from liver fibrogenesis. *Nat Commun* 2017;8:895.
- [15] Géraud C, Koch P-S, Zierow J, Klapproth K, Busch K, Olsavszky V, et al. GATA4-dependent organ-specific endothelial differentiation controls liver development and embryonic hematopoiesis. *J Clin Invest* 2017;127:1099–1114.
- [16] R Core Team. R: A Language and Environment for Statistical Computing. Vienna, Austria: R Foundation for Statistical Computing; 2019.
- [17] Géraud C, Schledzewski K, Demory A, Klein D, Kaus M, Peyre F, et al. Liver sinusoidal endothelium: a microenvironment-dependent differentiation program in rat including the novel junctional protein liver endothelial differentiation-associated protein-1. *Hepatology* 2010;52:313–326.
- [18] Kress TR, Pellanda P, Pellegrinet L, Bianchi V, Nicoli P, Doni M, et al. Identification of MYC-dependent transcriptional programs in oncogene-addicted liver tumors. *Cancer Res* 2016;76:3463–3472.
- [19] Ding B-S, Nolan DJ, Butler JM, James D, Babazadeh AO, Rosenwaks Z, et al. Inductive angiocrine signals from sinusoidal endothelium are required for liver regeneration. *Nature* 2010;468:310–315.
- [20] Ramachandran P, Dobie R, Wilson-Kanamori JR, Dora EF, Henderson BEP, Luu NT, et al. Resolving the fibrotic niche of human liver cirrhosis at single-cell level. *Nature* 2019;575:512–518.
- [21] Nie Z, Hu G, Wei G, Cui K, Yamane A, Resch W, et al. c-Myc is a universal amplifier of expressed genes in lymphocytes and embryonic stem cells. *Cell* 2012;151:68–79.
- [22] Bjarnegård M, Enge M, Norlin J, Gustafsson S, Fredriksson S, Abramsson A, et al. Endothelium-specific ablation of PDGFB leads to pericyte loss and glomerular, cardiac and placental abnormalities. *Development* 2004;131:1847–1857.

- [23] Czochra P, Klopčić B, Meyer E, Herkel J, García-Lazaro JF, Thieringer F, et al. Liver fibrosis induced by hepatic overexpression of PDGF-B in transgenic mice. *J Hepatol* 2006;45:419–428.
- [24] Raines SM, Richards OC, Schneider LR, Schueler KL, Rabaglia ME, Oler AT, et al. Loss of PDGF-B activity increases hepatic vascular permeability and enhances insulin sensitivity. *Am J Physiol Endocrinol Metab* 2011;301:E517–E526.
- [25] **Wilhelm A, Aldridge V, Haldar D, Naylor AJ, Weston CJ, Hedegaard D, et al.** CD248/endosialin critically regulates hepatic stellate cell proliferation during chronic liver injury via a PDGF-regulated mechanism. *Gut* 2016;65:1175–1185.
- [26] **Dobie R, Wilson-Kanamori JR, Henderson BEP, Smith JR, Matchett KP, Portman JR, et al.** Single-cell transcriptomics uncovers zonation of function in the mesenchyme during liver fibrosis. *Cell Rep* 2019;29:1832–1847.e8.
- [27] **Fan W, Liu T, Chen W, Hammad S, Longerich T, Haussler I, et al.** ECM1 prevents activation of transforming growth factor β , hepatic stellate cells, and fibrogenesis in mice. *Gastroenterology* 2019;157:1352–1367.e13.
- [28] **Xu M, Xu H-H, Lin Y, Sun X, Wang L-J, Fang Z-P, et al.** LECT2, a ligand for Tie1, plays a crucial role in liver fibrogenesis. *Cell* 2019;178:1478–1492.e20.
- [29] Sullivan MM, Barker TH, Funk SE, Karchin A, Seo NS, Höök M, et al. Matricellular hevin regulates decorin production and collagen assembly. *J Biol Chem* 2006;281:27621–27632.
- [30] **Xiong X, Kuang H, Ansari S, Liu T, Gong J, Wang S, et al.** Landscape of intercellular crosstalk in healthy and NASH liver revealed by single-cell secretome gene analysis. *Mol Cell* 2019;75:644–660.e5.
- [31] Toshikuni N, Ozaki K, George J, Tsutsumi M. Serum endocan as a survival predictor for patients with liver cirrhosis. *Can J Gastroenterol Hepatol* 2015;29:427–430.
- [32] Sokolović A, Sokolović M, Boers W, Elferink RPO, Bosma PJ. Insulin-like growth factor binding protein 5 enhances survival of LX2 human hepatic stellate cells. *Fibrogenesis Tissue Repair* 2010;3:3.
- [33] Hammoutene A, Rautou P-E. Role of liver sinusoidal endothelial cells in non-alcoholic fatty liver disease. *J Hepatol* 2019;70:1278–1291.
- [34] **Malehmir M, Pfister D, Gallage S, Szydłowska M, Inverso D, Kotsilitsi E, et al.** Platelet GPIb α is a mediator and potential interventional target for NASH and subsequent liver cancer. *Nat Med* 2019;25:641–655.